

BASIC SCIENCES

Development of Zafirlukast Analogues for Improved Antithrombotic Activity Through Thiol Isomerase Inhibition

Justine A. Keovilay, Kaitlind C. Howard, Kirk A. Taylor¹, Sabeeya Khan¹, Sienna E. Wurl, Melanie K. Szahaj, Tanya Sage¹, Nishad Thamban Chandrika¹, Caixia Hou¹, Oleg V. Tsodikov, Jonathan M. Gibbins¹, Sylvie Garneau-Tsodikova¹, Daniel R. Kennedy¹

BACKGROUND: Thiol isomerases play essential and nonredundant roles in platelet activation, aggregation, and thrombus formation. Thiol isomerase inhibitors have the potential to overcome the 2 major drawbacks of current antithrombotic therapies, as they target both arterial and venous thrombosis without enhancing bleeding risks. Recently, a Food and Drug Administration–approved drug, zafirlukast (ZAF), was shown to be a promising pan-thiol isomerase inhibitor. The objective of this study is to develop analogues of ZAF with optimized thiol isomerase inhibition and antithrombotic activity.

METHODS: Thirty-five ZAF analogues were tested in an insulin turbidometric assay for thiol isomerase inhibition. Analogues were tested for platelet activation, aggregation, P-selectin expression, and laser-induced thrombosis in mice and compared with the parent compound.

RESULTS: Of the 35 analogues, 12 retained activity, with 1, compound 21, that demonstrated a greater potency than that of ZAF, 5 had a similar potency to that of ZAF, and 6 had a weaker potency. Analogues demonstrated inhibition of platelet aggregation and P-selectin expression as compared with ZAF, consistent with their potencies. ZAF and compound 21 were shown to be reversible inhibitors of thiol isomerases, and not cytotoxic to cultured, lung, liver, and kidney cells. Finally, in an in vivo assessment of thrombus formation, compound 21 was able to significantly inhibit thrombus formation without affecting bleeding times.

CONCLUSIONS: A ZAF analogue, compound 21, with properties superior to those of ZAF was synthesized, demonstrating improved inhibition of platelet activation, aggregation, and thrombus formation as compared with the parent ZAF. This approach could yield a promising clinical candidate for treatment and prophylaxis of arterial and venous thrombosis.

GRAPHIC ABSTRACT: A [graphic abstract](#) is available for this article.

Key Words: drug repositioning ■ isomerases ■ protein disulfide-isomerases ■ structure-activity relationship ■ thrombosis

Thrombosis is the most common underlying pathology related to diseases such as myocardial infarction, stroke, ischemic heart disease, deep vein thrombosis, and pulmonary embolism.^{1–3} Yet, despite the prevalence of these diseases, current antithrombotic agents cannot prevent both arterial^{4,5} and venous thrombosis,^{6,7} and they are associated with significant risks of bleeding, limiting their prophylactic use.⁸

Thiol isomerase inhibitors have the potential to overcome these 2 major limitations to current therapy, as they have the ability to target both arterial and venous thrombosis without an increased risk of bleeding.^{2,9} Indeed, a clinical study of patients with advanced cancer taking isoquercetin, a selective inhibitor of the thiol isomerase PDI (protein disulfide isomerase), demonstrated decreased platelet-dependent thrombin and

Correspondence to: Daniel R. Kennedy, PhD, Department of Pharmaceutical and Administrative Sciences, College of Pharmacy and Health Sciences, Western New England University, 1215 Wilbraham Rd, Springfield, MA 01119. Email dkennedy@wne.edu

Supplemental Material is available at <https://www.ahajournals.org/doi/suppl/10.1161/ATVBAHA.124.321579>.

For Sources of Funding and Disclosures, see page e148.

© 2025 American Heart Association, Inc.

Arterioscler Thromb Vasc Biol is available at www.ahajournals.org/journal/atvb

Nonstandard Abbreviations and Acronyms

CRP	collagen-related peptide
CysLTR	cysteinyl leukotriene receptor
DMSO	dimethyl sulfoxide
ERp57	endoplasmic reticulum-resident protein 57
ERp72	endoplasmic reticulum-resident protein 72
HRP	horseradish peroxidase
PDI	protein disulfide isomerase
PE	phycoerythrin
PRP	platelet-rich plasma
SAR	structure-activity relationship
ZAF	zafirlukast

circulating soluble P-selectin levels without enhanced bleeding.¹⁰ Thiol isomerases have extracellular activities that modulate thrombus formation, fibrin formation, and platelet aggregation.^{11–13} These enzymes include PDI and closely related endoplasmic reticulum-resident proteins ERp57¹⁴ (endoplasmic reticulum-resident protein 57) and ERp72¹⁵ (endoplasmic reticulum-resident protein 72), which play important roles in both arterial and venous thrombosis through the propagation of platelet activation.¹⁶ Inhibition of these enzymes has been shown to decrease platelet activation, aggregation, and adhesion, in addition to inhibiting thrombus formation.^{17,18} Interestingly, these enzymes are nonredundant, as a genetic deletion of 1 thiol isomerase family member, while rescued by the respective recombinant enzyme, is not rescued by other family members,^{19–22} suggesting that pan-thiol isomerase inhibitors may have additional effects compared with selective PDI inhibitors.

Previously, we identified zafirlukast (ZAF), a Food and Drug Administration–approved CysLTR (cysteinyl leukotriene receptor) 1 antagonist used for the treatment of asthma,²³ as a pan inhibitor of thiol isomerase activity.² ZAF was shown to modulate platelet function and integrin function *ex vivo*, including inhibiting platelet aggregation and P-selectin expression while also demonstrating *in vivo* inhibition of thrombus formation in live mice.² In a previous study, we demonstrated that an analogue of ZAF that lacked the moiety involved in binding the CysLTR1 receptor retained thiol isomerase inhibitory activity.²⁴ Thus, ZAF analogue optimization by medicinal chemistry may yield an analogue with improved potency as a thiol isomerase inhibitor and no activity as a CysLTR1 antagonist. The structure of ZAF offers a rich opportunity for structure-activity relationship (SAR) studies, as its molecular structure contains a cyclopentyl carbamate attached to an *N*-methylindole and an arylsulfonamide scaffold linked via a decorated benzoyl ring (Figure 1). These chemical moieties suggest various modification possibilities for SAR studies, including varying the identities and

Highlights

- Zafirlukast analogues inhibit thiol isomerases broadly and reversibly.
- Zafirlukast analogues improve inhibition of platelet aggregation.
- Zafirlukast analogues inhibit *in vivo* thrombus formation and decrease thrombus stability.
- Zafirlukast analogues do not affect bleeding times in mice.

positions of the substituents on each of these aromatic and heterocyclic ring systems and altering scaffold organization, with the goal of increasing the inhibition of thiol isomerases and detuning the inhibition of CysLTR1.^{25,26} Previously, SAR studies of ZAF were successful in developing potent antibacterial ZAF analogues to combat the periodontal disease^{25,26}; therefore, there is the potential to develop improved analogues that target thiol isomerases for thrombosis prevention and treatment.

In this study, we investigated 35 ZAF analogues to identify modifications that improve thiol isomerase inhibition potency. Select analogues were explored for their ability to inhibit platelet aggregation and P-selectin expression. The most promising lead compound 21 was explored for its ability to reversibly inhibit thiol isomerases, block surface thiols, inhibit *in vivo* thrombus formation, and its effect on bleeding times.

MATERIALS AND METHODS

Data Availability Statement

The data generated in this study are available upon request to the corresponding author.

Reagents

Recombinant human ERp57, PDI, and ERp72 were purchased from Abcam (Cambridge, MA). ZAF was purchased from TCI America (Portland, OR). Recombinant insulin (bovine), dithiothreitol (DTT), buffers, and all other chemicals were purchased from Sigma-Aldrich (St. Louis, MO) and Avantor (Radnor, PA). The 96- and 384-well clear bottom plates were purchased from Corning (NY).

Chemical Synthesis

The ZAF analogues were synthesized as described previously.^{25,27}

Insulin-Based Turbidometric Assay

Initially, the potency of the ZAF analogues in inhibiting thiol isomerase activity was determined by an insulin turbidity assay using ERp57, as previously described.² Briefly, the analogues were diluted at specified concentrations for a 5-point dose-response curve in a 384-well plate, and the reactions were run at 37 °C

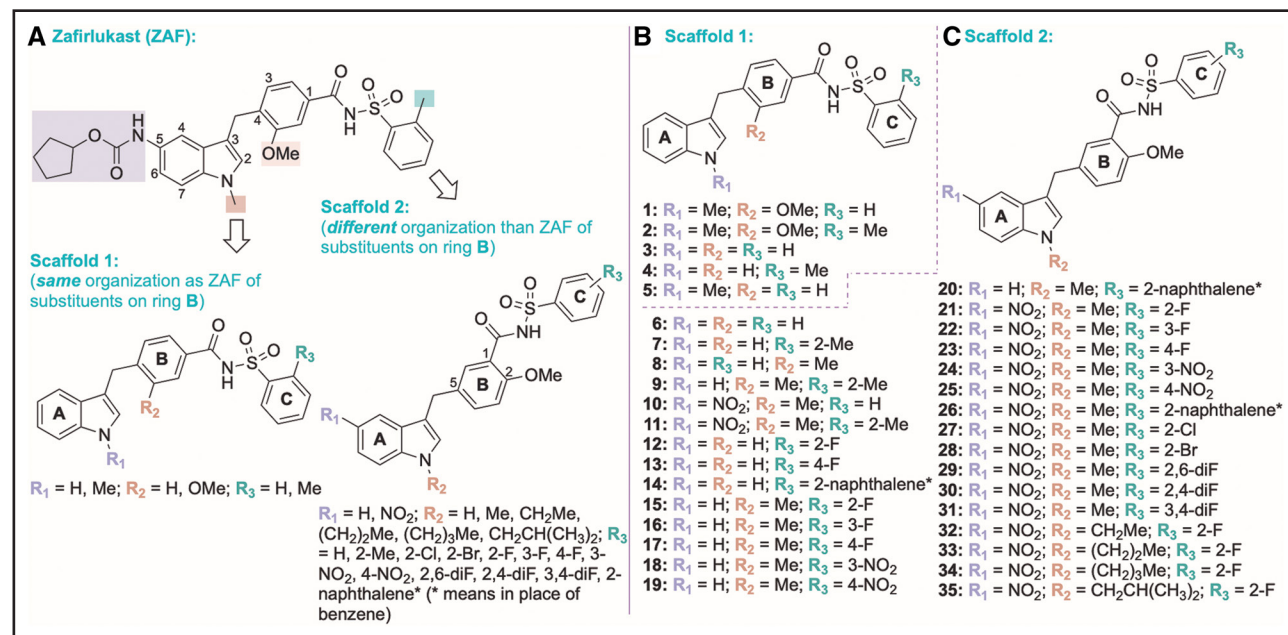


Figure 1. The structures of zafirlukast (ZAF) and its 35 analogues tested in this study.

A, The structures of ZAF and the 2 chemical scaffolds of the synthesized ZAF derivatives. **B,** The ZAF analogues with scaffold 1. **C,** The ZAF analogues with scaffold 2.

with final concentrations of 20 $\mu\text{g/mL}$ (350 nmol/L) ERp57 and 125 $\mu\text{mol/L}$ insulin in the reaction buffer (100 mmol/L potassium phosphate, pH 7.4, adjusted at room temperature, 2 mmol/L EDTA) in a total volume of 30 μL per well. The reaction was initiated with 0.3 mmol/L DTT, and the turbidity of insulin aggregation was monitored by measuring absorbance at 650 nm every minute for 90 minutes using the SpectraMax M3 plate reader (Molecular Devices, Sunnyvale, CA). The same procedure was used to measure inhibition of PDI and ERp72 by compound 21, substituting ERp57 for the enzyme of interest. Experiments were performed in quadruplicate.

To determine the reversibility of inhibition, ZAF, compound 21, the reversible control rutin,⁹ and the irreversible control PACMA-31²⁸ (PACMA; propynoic acid carbamoyl methyl amide) were preincubated with 180 nmol/L PDI at a final concentration of 30 $\mu\text{mol/L}$ in the same reaction buffer for 0, 0.5, 1, or 4 hours. Then, the reactions were initiated by the addition of 125 $\mu\text{mol/L}$ insulin and 0.3 mmol/L DTT, and the turbidity was measured for 90 minutes. Dimethyl sulfoxide (DMSO; 1%) was used as a control. Experiments for ZAF and compound 21 were performed in triplicate.

Inhibitor-Binding Assay

ERp57 (1 $\mu\text{mol/L}$) was mixed with compound 21 at specified concentrations in binding buffer (100 mmol/L potassium phosphate, pH 7.4, 2 mmol/L EDTA, 0.3 mmol/L DTT) on ice. The enzyme without inhibitors was mixed with DMSO as a control. The samples were loaded into a 96-well plate at 21 $^\circ\text{C}$, the intrinsic fluorescence of protein tryptophan residues was measured using the excitation wavelength of 290 nm with a cutoff filter at 325 nm and the emission scanned at the wavelengths of 325 to 380 nm. At these conditions, the contribution of compound 21 to the measured fluorescence was negligible compared with that of the protein at all concentrations of the

inhibitor used in this assay. The titrations were performed in triplicate. Relative fluorescence quenching ($|\Delta\omega|/\omega_0$, the fraction of fluorescence lost) at the fluorescence maximum (339 nm) was plotted as a function of inhibitor concentration and used in a nonlinear regression analysis with SigmaPlot 9.0 (Grafitti) with the following 1:1 binding isotherm, to obtain the values of the equilibrium binding constant K_d :

$$\frac{|\Delta\omega|}{\omega_0} = A \frac{[I]}{K_d + [I]}$$

Here, A is the relative fluorescence quenching at infinite inhibitor concentration, the second fitting parameter.

Cytotoxicity Assay

Human embryonic kidney (HEK-293), human bronchial epithelial (BEAS-2B), and hepatocyte carcinoma (HepG2) cells were plated in 96-well microtiter plates at concentrations of 10 000 cells per well for HEK-293 and 3000 cells per well for BEAS-2B and HepG2. The plates were incubated with 5% CO_2 at 37 $^\circ\text{C}$ for 16 hours to allow the cells to adhere to the wells. The medium was removed, and fresh medium with ZAF or analogue 21 was added. Negative control contained 0.1% DMSO, and the positive control contained 1% Triton X-100. The relative cell survival was evaluated after 24 hours of incubation by adding resazurin (10 μL of 10 mmol/L solution) for 6 hours. The SpectraMax M5 plate reader was used to monitor live cells by fluorescence measurements with 560 nm excitation and 590 nm emission wavelengths and the relative cell survival values were then calculated. Experiments were performed in quadruplicate.

Platelet Preparation and Stimulation

After receiving approval from the Western New England University institutional review board, human platelets were collected from

consenting, drug-free donors in tubes containing 3.2% sodium citrate using standard venipuncture techniques. Platelet-rich plasma (PRP) was obtained by centrifugation of whole blood at 100g for 20 minutes at 20 °C. For washed platelets, 10 µL of 125 µg/mL prostacyclin was added to PRP and centrifuged at 1410g for 10 minutes at 20 °C. The supernatant was removed and platelets were resuspended in 1 mL of Tyrode buffer (20 mmol/L HEPES, 144 mmol/L NaCl, 3 mmol/L KCl, 12 mmol/L NaHCO₃, and 1 mmol/L MgCl₂, pH 7.3, adjusted at room temperature) and 150 µL acid citrate dextrose (97 mmol/L Na₃C₆H₅O₇, 111 mmol/L C₆H₁₂O₆, and 78 mmol/L C₆H₈O₇) with an additional 21 mL Tyrode buffer, 3 mL acid citrate dextrose, and 10 µL of 125 µg/mL prostacyclin added to the suspension. Platelets were then centrifuged at 1410g for 10 minutes at 20 °C, the supernatant removed, and the platelet pellet resuspended in Tyrode buffer. For aggregation assays, PRP was incubated with vehicle (DMSO, 0.1% v/v in Tyrode buffer), ZAF (1.25, 2.5, 5, 10, 20, or 40 µmol/L), compound 21 (1.25, 2.5, 5, 10, or 20 µmol/L), compound 22, or compound 35 (1.25, 2.5, 5, 10, 20, 40, or 80 µmol/L) for 5 minutes before stimulation. Then, collagen (1.9 mg/mL diluted in water) was used to stimulate platelets for 180 s in a lumi-aggregometer (PAP-8E, Horsham, PA) with continuous stirring. The experiments were performed in quadruplicate.

P-Selectin Exposure

To assess P-selectin exposure on platelets, 46 µL of HEPES buffered saline (10 mmol/L HEPES, pH 7.4, adjusted at room temperature, 134 mmol/L NaCl, 5 mmol/L KCl, 2 mmol/L MgSO₄), 2 µL of PRP and PE (phycoerythrin) conjugated anti-CD62P (1:50 dilution from the purchased stock; BD Biosciences; catalog No. 551142), or PE conjugated IgG1 isotype control (1:50 dilution from the purchased stock; BD Biosciences, Franklin Lakes, NJ; catalog No. 555750) were incubated with vehicle control (DMSO, 0.1% v/v in Tyrode buffer), ZAF, compound 21, compound 22, or compound 35 (0, 3, 10, and 30 µmol/L) for 30 minutes at room temperature. Upon completion of incubation, platelets were stimulated with CRP (collagen-related peptide; 5 µg/mL) and allowed to incubate for an additional 30 minutes at room temperature. The platelets were then fixed with 100 µL of 0.2% formalin. The platelets were analyzed on a BD Accuri C6 Plus flow cytometer for P-selectin expression with 10 000 gated events recorded. The experiments were performed in triplicate.

3-(N-Maleimidylpropionyl)-Biocytin Thiol Labeling and Blotting

Washed platelets were treated with vehicle control (DMSO, 0.1% v/v in Tyrode buffer), 20 µmol/L ZAF, or 20 µmol/L compound 21 for 5 minutes, then stimulated in the same manner as above. Then 250 µL of drug-treated stimulated platelets were incubated with 100 µmol/L 3-(N-maleimidopropionyl)-biocytin (Cayman Chemical, Ann Arbor, MI) for 20 minutes at 37 °C, and then with excess DTT to quench any unbound 3-(N-maleimidopropionyl)-biocytin. After incubation, 50 µL of SDS-PAGE sample loading buffer containing 125 mmol/L DTT (Cell Signaling Technology, Danvers, MA) was added to each sample, heated for 5 minutes at 95 °C, and then put on ice. Of each sample, 25 µL was then analyzed by SDS-PAGE using the Bio-Rad mini gel system (Bio-Rad, Hercules, CA) in SDS-PAGE running buffer (25 mmol/L Tris, 192 mmol/L glycine,

0.1% SDS, pH 8.3) and transferred to a polyvinylidene difluoride membrane in transfer buffer (25 mmol/L Tris, 192 mmol/L glycine, 20% methanol). After transfer, membranes were blocked for 1 hour at room temperature in blocking buffer (Tris-buffered saline [15 mmol/L Tris-HCL, 4.6 mmol/L Tris-base, 150 mmol/L NaCl, pH 7.6, adjusted at room temperature]+5% nonfat dry milk, w/v), then probed with streptavidin-HRP (horseradish peroxidase) conjugate (Thermo Fisher Scientific, Waltham, MA) in a 1:5000 dilution in Tris-buffered saline+0.1% Tween-20 and chemiluminescence detected with Novex ECL substrate (Invitrogen, Waltham, MA) on a Bio-Rad ChemiDoc Imaging System (Bio-Rad). Membranes were stripped in buffer (200 mmol/L glycine, 3.5 mmol/L SDS, 1% Tween-20, pH 2.2, adjusted at room temperature) and reprobed with a β-actin primary antibody (1:5000 dilution; Cell Signaling Technology) followed by an HRP-coupled secondary antibody (1:10 000 dilution; Cell Signaling Technology) and chemiluminescence detected as described above. Membranes were analyzed using the Bio-Rad Image Lab software (Bio-Rad). Experiments were performed in quadruplicate.

Assessment of Thrombus Formation, Emboli Formation, and Tail Bleeding in Mice

To assess the ability of compound 21 to inhibit in vivo arterial thrombus formation, intravital microscopy using laser injury was performed. Male C57BL/6J mice aged 4 to 6 weeks with a weight range of 19 to 28 g were anaesthetized by intraperitoneal injection of ketamine (100 mg/kg), medetomidine (1.0 mg/kg), and atropine (0.25 mg/kg) and maintained at 37 °C throughout the duration of the experiment. Platelets were labeled via intravenous infusion of DyLight 649-conjugated anti-glycoprotein Ib platelet labeling antibody (EmFret Analytics, Wurzburg, Germany; 0.2 µg/g of body weight) as previously reported.² After the exposure of the testicular cremaster muscle, the vehicle DMSO in Tyrode buffer (0.1% v/v) or compound 21 was infused intravenously. Then, following a 5-minute incubation period, the arterial wall injury was induced by laser ablation (Micropoint; Andor Technology, Belfast, United Kingdom). Thrombus formation was observed with the Olympus BX microscope (Olympus, Essex, United Kingdom) at ×60 magnification and a Hamamatsu CCD (charge-coupled device) camera (Hamamatsu Photonics, Hertfordshire, United Kingdom). The data were analyzed using Slidebook 2023 (Intelligent Imaging Innovations, Denver, CO).^{14,15,29} Thrombus formation data were smoothed using LOWESS (locally weighted scatterplot smoothing) curves within GraphPad Prism to calculate maximum fluorescence intensity for each thrombus. Emboli were recorded using an empty mask that was positioned downstream of the thrombus when the field of view allowed. An embolic event was classified as a transient recording of a platelet mass within this gate and was visually confirmed by the experimenter. The experiments were performed with 5 separate mice per group, where multiple thrombi were able to be formed per mouse. Only male mice were used in these experiments due to the location of arterial injury at the cremaster muscle, of which only male mice have this anatomic feature. Mice were euthanized using Schedule 1-approved methods (cervical dislocation) at the end of the experiment. For the tail bleeding assay, male C57BL/6J mice (n=10 per group) were anaesthetized by intraperitoneal injection of ketamine and medetomidine, and compound 21

or vehicle was infused into the femoral vein 5 minutes before tail biopsy. Following drug treatment, 0.2 cm of the tail tip was excised and blood collected into sterile PBS. Time to bleeding cessation was recorded. Mice were euthanized when bleeding had ceased or at 20 minutes post-tail tip excision. All animal experiments were blinded for both the experimental treatment and the analysis. The animal experiments were approved by the University of Reading Local Ethical Review Panel and authorized by the UK Home Office.

Statistics

The statistical analyses were performed using GraphPad Prism (version 9.4.0; San Diego, CA). Data were presented as the mean \pm SD. For reversibility, platelet aggregation, and P-selectin studies, a 2-way ANOVA with a Tukey post hoc test was used as each mean was compared with every other mean. For the 3-(*N*-maleimidopropionyl)-biocytin thiol labeling study, a 1-way ANOVA with a Tukey post hoc test was performed. For in vivo thrombus formation and tail bleed assays, a Mann-Whitney *U* test was performed as data were not normally distributed.

RESULTS

SAR Analysis of ZAF Analogues for Thiol Isomerase Inhibition

The 35 ZAF analogues evaluated in this study consist of 1 of 2 major scaffolds, 1 and 2 (Figure 1). In scaffold 1, the organization of the substituents on the benzoyl group (ring B) was kept the same as that found in the parent ZAF (3-methoxy-4-indoyl organization), while in scaffold 2, the organization of the substituents on ring B was different (2-methoxy-5-indoyl organization). The use of 2 different scaffolds offered an ideal opportunity for initial SAR studies. Of note, none of these ZAF analogues contained the cyclopentyl moiety appended to ring A in ZAF. The removal of the cyclopentyl moiety resulted in a >100-fold reduction in potency of ZAF analogues as CysLTR1 antagonists.³⁰ Moreover, the different organization of scaffold 2 from that of ZAF is expected to lead to further significant reduction or loss of CysLTR1 antagonism for the analogues with this scaffold. For this reason, 30 of the 35 analogues tested in this study belonged to scaffold 2.

To determine the potency of ZAF and its 35 analogues (1–35) as thiol isomerase inhibitors, we first tested all compounds for their inhibition of thiol isomerase ERp57 (Table; Figure 2A and 2B; Figure S1). In addition to ZAF, 11 analogues displayed concentration-dependent inhibition of ERp57 (Figure S1), while the rest of the analogues did not show observable inhibition up to 100 μ M/L. In addition to ZAF, only 1 of the analogues with scaffold 1 (compound 2) inhibited ERp57, but this inhibition was weak (IC_{50} =99 \pm 8 μ M/L). Note that IC_{50} in this study is defined as the inhibitor concentration at which the enzyme is inhibited by 50% of its activity in the absence of an inhibitor, regardless of whether the inhibitor can completely inhibit the enzyme or not. In analogue 2, the identities of R_1 , R_2 , and R_3 groups all

Table. The Potencies of ZAF Analogues as ERp57 Inhibitors

Active compounds					
Compound	Scaffold	R ₁	R ₂	R ₃	IC ₅₀ , μ M
ZAF					25 \pm 4*
2	1	Me	OMe	Me	99 \pm 8†
21	2	NO ₂	Me	2-F	9.9 \pm 1.1*
22	2	NO ₂	Me	3-F	33 \pm 9†
23	2	NO ₂	Me	4-F	44 \pm 11†
24	2	NO ₂	Me	3-NO ₂	33 \pm 15†
26	2	NO ₂	Me	2-naphthalene in place of benzene	>100†
27	2	NO ₂	Me	2-Cl	61 \pm 9†
28	2	NO ₂	Me	2-Br	50 \pm 14†
31	2	NO ₂	Me	3,4-diF	>100†
34	2	NO ₂	(CH ₂) ₃ Me	2-F	40 \pm 15†
35	2	NO ₂	CH ₂ CH(CH ₃) ₂	2-F	>100†
Inactive compounds					
1	1	Me	OMe	H	...‡
3	1	H	H	H	...
4	1	H	H	Me	...
5	1	Me	H	H	...
6	2	H	H	H	...
7	2	H	H	2-Me	...
8	2	H	Me	H	...
9	2	H	Me	2-Me	...
10	2	NO ₂	Me	H	...
11	2	NO ₂	Me	2-Me	...
12	2	H	H	2-F	...
13	2	H	H	4-F	...
14	2	H	H	2-naphthalene in place of benzene	...
15	2	H	Me	2-F	...
16	2	H	Me	3-F	...
17	2	H	Me	4-F	...
18	2	H	Me	3-NO ₂	...
19	2	H	Me	4-NO ₂	...
20	2	H	Me	2-naphthalene in place of benzene	...
25	2	NO ₂	Me	4-NO ₂	...
29	2	NO ₂	Me	2,6-diF	...
30	2	NO ₂	Me	2,4-diF	...
32	2	NO ₂	CH ₂ Me	2-F	...
33	2	NO ₂	(CH ₂) ₂ Me	2-F	...

ERp57 indicates endoplasmic reticulum-resident protein 57; and ZAF, zafirlukast.

*The corresponding dose-response data for these compounds are presented in Figure 2A and 2B.

†The corresponding dose-response data for these compounds are presented in Figure S1.

‡The ellipsis indicates that no inhibition was detected even at the highest concentration of 100 μ M/L of compound tested.

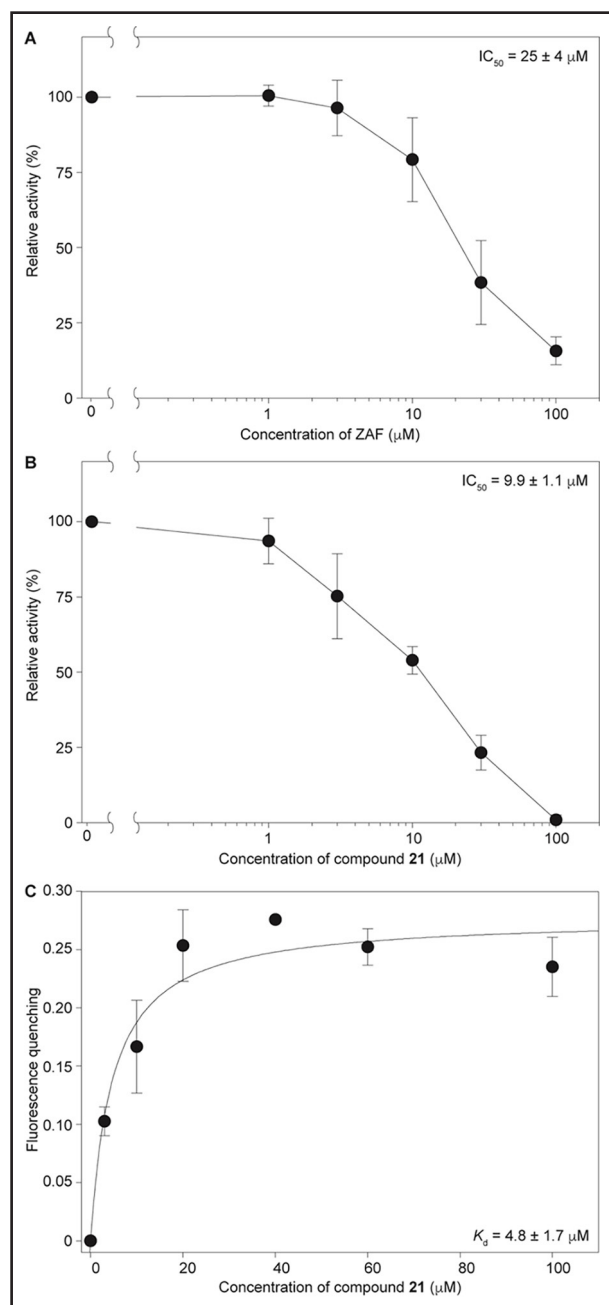


Figure 2. Enzymatic inhibition of ERp57 activity by zafirlukast and compound 21.

Dose-response data for (A) zafirlukast (ZAF) and (B) compound 21 in the turbidometric ERp57 (endoplasmic reticulum-resident protein 57) activity assay. The corresponding IC_{50} values are shown in the insets and presented in the Table. **C**, The binding isotherm for the formation of compound 21–ERp57 complex, obtained by monitoring quenching of fluorescence of ERp57's tryptophan residues. The K_d value obtained by the nonlinear regression using the 1:1 binding model is given in the inset.

matched those of ZAF, whereas other analogues with scaffold 1, in which these groups were replaced by hydrogens, were inactive as ERp57 inhibitors.

Among the 10 active analogues with scaffold 2, one (compound 21) was 2.5-fold more potent than ZAF

(Figure 2A and 2B), indicating that the inhibition of ERp57 could be uncoupled from CysLTR1 antagonism. The other 9 analogues were similarly potent or less potent than ZAF (Figure S1). Six of these compounds (compounds 22, 23, 24, 27, 28, and 34) had comparable or, at most, ≈ 2 -fold weaker inhibition potencies relative to that of ZAF. The other 3 compounds, 26, 31, and 35, were weak inhibitors. These observations indicated that a 2-F was the most preferred substitution at the R_3 position (in the context of $R_1=NO_2$ and $R_2=Me$), among those tested, whereas the bulkier and nonpolar 2-Cl (compound 27) and 2-Br (compound 28) were inferior. A 3-F, 3- NO_2 , or a 4-F at the R_3 position (compounds 22, 24, and 23) were tolerable, but these substituents did not yield potency improvement. With a 2-F at the R_3 and an NO_2 at the R_1 position, increasing the size of an alkyl substituent at the R_2 position (as in compounds 33, 34, and 35) decreased or abolished inhibition potency, although an *n*-butyl group at the R_2 position (compound 34) was tolerable. These compounds contained either 4-F or the polar 3- NO_2 substitutions at the R_3 position or a bulky naphthalene ring in place of the benzene ring. Compounds with other substitutions tested at the R_3 position, including di-F substitutions, were not inhibitory to ERp57. Identities of the groups at the R_1 and R_2 positions were not as varied as the R_3 position in this compound set. Compounds with unsubstituted R_1 and R_2 positions were inactive as ERp57 inhibitors.

Next, we tested the direct binding of the most potent inhibitor (compound 21) to ERp57. We monitored quenching of intrinsic fluorescence of ERp57, originated mostly from its tryptophan (Trp) residues, upon titrating compound 21 (Figure 2C). A significant (25%) saturable quenching signal was observed, consistent with specific binding, yielding the value of the equilibrium binding constant of $4.8 \pm 1.7 \mu\text{mol/L}$, in agreement with the IC_{50} of this compound. Compound 21 was additionally tested for its inhibition of thiol isomerases PDI and ERp72 (Figure S2). Compound 21 inhibited both of these enzymes with an $IC_{50} \approx 20 \mu\text{mol/L}$, about 2-fold less potently than it did ERp57.

Reversibility of ZAF Analogues

The reversibility of potential antithrombotic agents is an important property due to the potential risks from bleeding. Although ZAF did not display enhanced bleeding risk in mice,² the reversibility of thiol isomerase inhibition by ZAF and its analogues has not previously been examined. The reversibility of thiol isomerases can be explored using a modified version of the insulin-based turbidometric assay, as previously shown by Jasuja et al.⁹ Because ZAF and compound 21 are pan-thiol isomerase inhibitors, we chose to use PDI to examine the reversibility of these compounds, because reversible (rutin)⁹ and irreversible (PACMA)²⁸ inhibitors of this enzyme are known

and could be used as controls. An irreversible inhibitor inhibits the enzymatic reaction in a preincubation time-dependent manner, as demonstrated by PACMA (Figure 3A). On the contrary, a fast reversible inhibitor binds and dissociates from the protein dynamically, demonstrating similar levels of inhibition independent of preincubation time, as evidenced by rutin (Figure 3B). Both ZAF and compound 21 (Figure 3C and 3D) displayed no preincubation time dependence for all 4 time points, consistent with the effects of reversible thiol isomerase inhibitors.

Platelet Aggregation and P-Selectin Assays of ZAF and Compound 21

Platelet aggregation was measured in PRP upon 180 s stimulation with collagen in the presence of 0.1% DMSO, ZAF (1.25–40 $\mu\text{mol/L}$; Figure 4A), or compound 21 (1.25–20 $\mu\text{mol/L}$; Figure 4B). ZAF and compound 21 inhibited platelet aggregation in a dose-dependent manner. The end point values for ZAF and compound 21 at 180 s from 4 respective independently replicated runs calculated relative to the DMSO

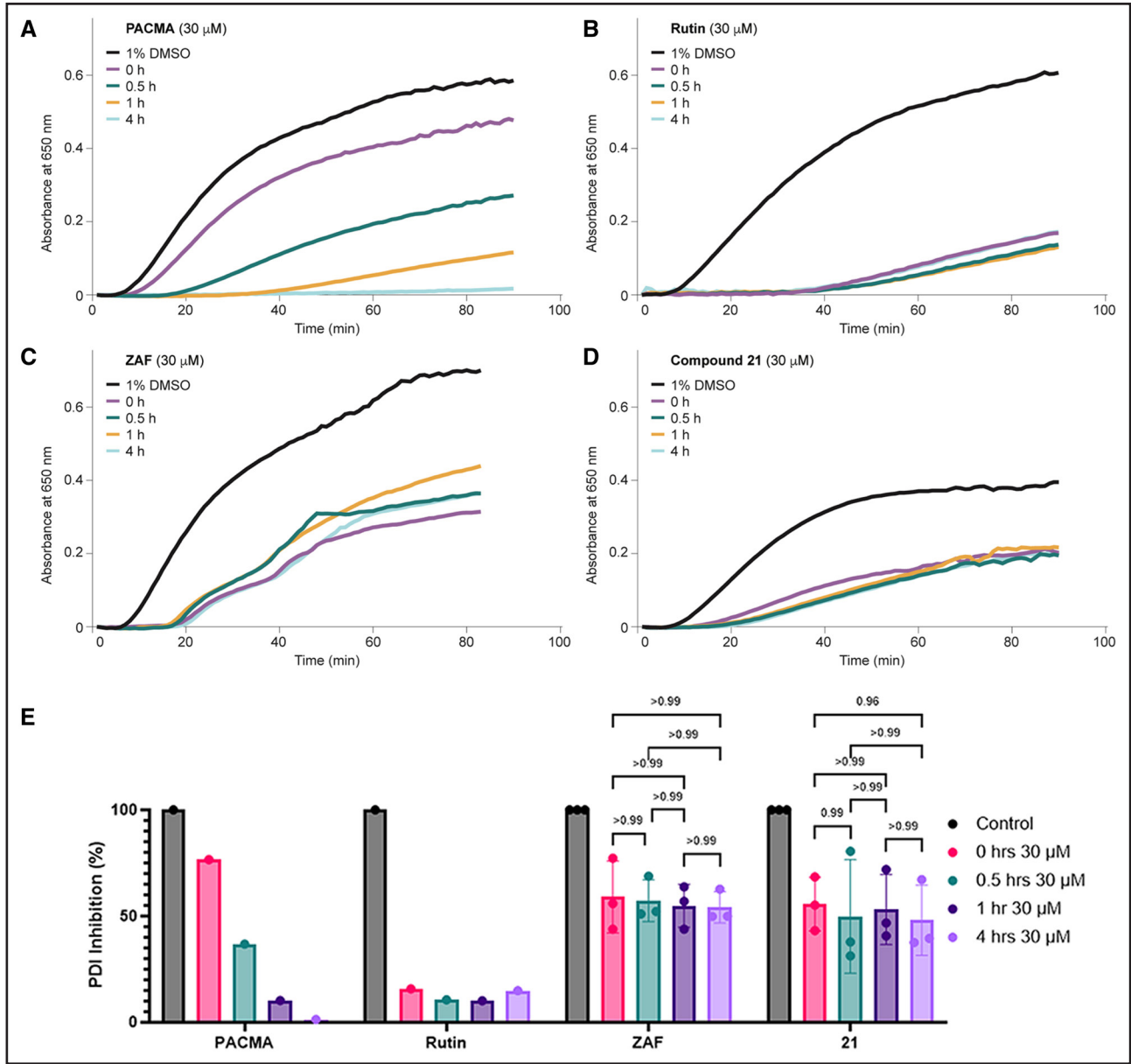


Figure 3. The turbidimetric insulin assay to test the pattern of reversibility for PDI (protein disulfide isomerase) inhibitors tested at 30 $\mu\text{mol/L}$ at 4 different time points up to 4 hours. **A**, Irreversible PDI inhibitor PACMA (propynoic acid carbamoyl methyl amide). **B**, Reversible PDI inhibitor rutin. **C**, Zafirlukast (ZAF). **D**, Compound 21. **E**, A bar graph depicting a summary of the 3 individual runs for 3 replicates of ZAF and compound 21 where no time-dependent change is seen. Data are presented as mean \pm SD. Statistical analysis: 2-way ANOVA with Tukey post hoc test.

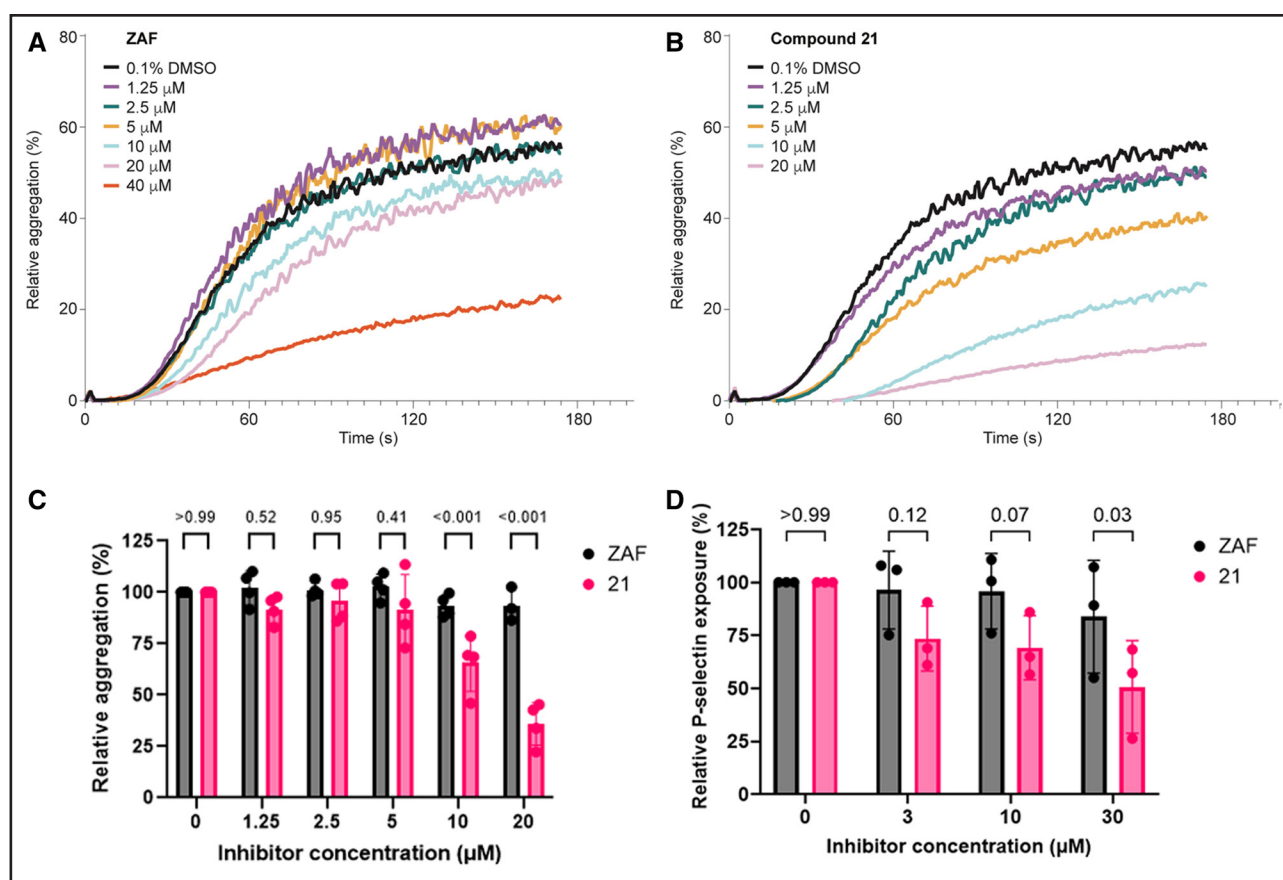


Figure 4. Inhibition of platelet aggregation and P-selectin exposure by zafirlukast (ZAF) and compound 21.

A through **C**, Platelet-rich plasma (PRP) was collected from consenting donors and incubated with indicated concentrations of ZAF, compound 21, or vehicle for 5 minutes at 37 °C. Platelet aggregation was induced by collagen (1.9 mg/mL), and representative traces of (**A**) ZAF and (**B**) compound 21 are presented. **C**, The end point aggregation values at 180 s for ZAF (n=4) and compound 21 (n=4). Data are presented as mean±SD. Statistical analysis: 2-way ANOVA with Tukey post hoc test. **D**, Flow cytometry measurement of P-selectin exposure from PRP treated with ZAF (n=3) or compound 21 (n=3) and stimulated with CRP (collagen-related peptide; 5 μg/mL). Data are presented as mean±SD. Statistical analysis: 2-way ANOVA with a Tukey post hoc test.

value are displayed in Figure 4C. Compound 21 continued to be more potent than ZAF, demonstrating 31% inhibition at 10 μmol/L, whereas ZAF inhibited platelet aggregation only by 7%. At 20 μmol/L, compound 21 and ZAF inhibited aggregation by 58% and 7%, respectively. A significant difference was seen between the 2 compounds at both 10 and 20 μmol/L (Figure 4C). When used at 10 μmol/L, compound 21 inhibited platelet aggregation similarly to 40 μmol/L ZAF (Figure 4A and 4B).

The ability of compound 21 to inhibit P-selectin activation was also tested (Figure 4D). Flow cytometry was utilized to assess the P-selectin exposure of PRP treated with ZAF or compound 21. Compound 21 was also more effective than ZAF at inhibiting P-selectin expression, demonstrating average inhibition of 27% versus 5% at 3 μmol/L, 32% versus 5% at 10 μmol/L, and 50% versus 17% at 30 μmol/L, with a significant difference observed between the effects of the 2 compounds at 30 μmol/L.

Correlation of Thiol Isomerase Activity to Antiplatelet Effects in Select Analogues

To test whether the observed effects of compound 21 on platelet aggregation and P-selectin exposure were through thiol isomerase inhibition, we explored whether additional ZAF analogues inhibited these assays at levels relative to their thiol isomerase inhibitory effect. Thus, the effects of compound 22, which had a similar inhibitory effect to ZAF in the insulin turbidity assay and compound 35, which was a weaker inhibitor than ZAF, were examined and compared with ZAF and compound 21 (Figure 5A). As expected, compound 22 had similar activity to ZAF in both platelet aggregation inhibition and P-selectin exposure, while compound 35 inhibited platelet aggregation less effectively (Figure 5B and 5C). Compound 35 displayed a similar inhibitory effect on P-selectin expression to that of ZAF and compound 22, but besides that, the overall activity of the compounds in the cell-based assays was

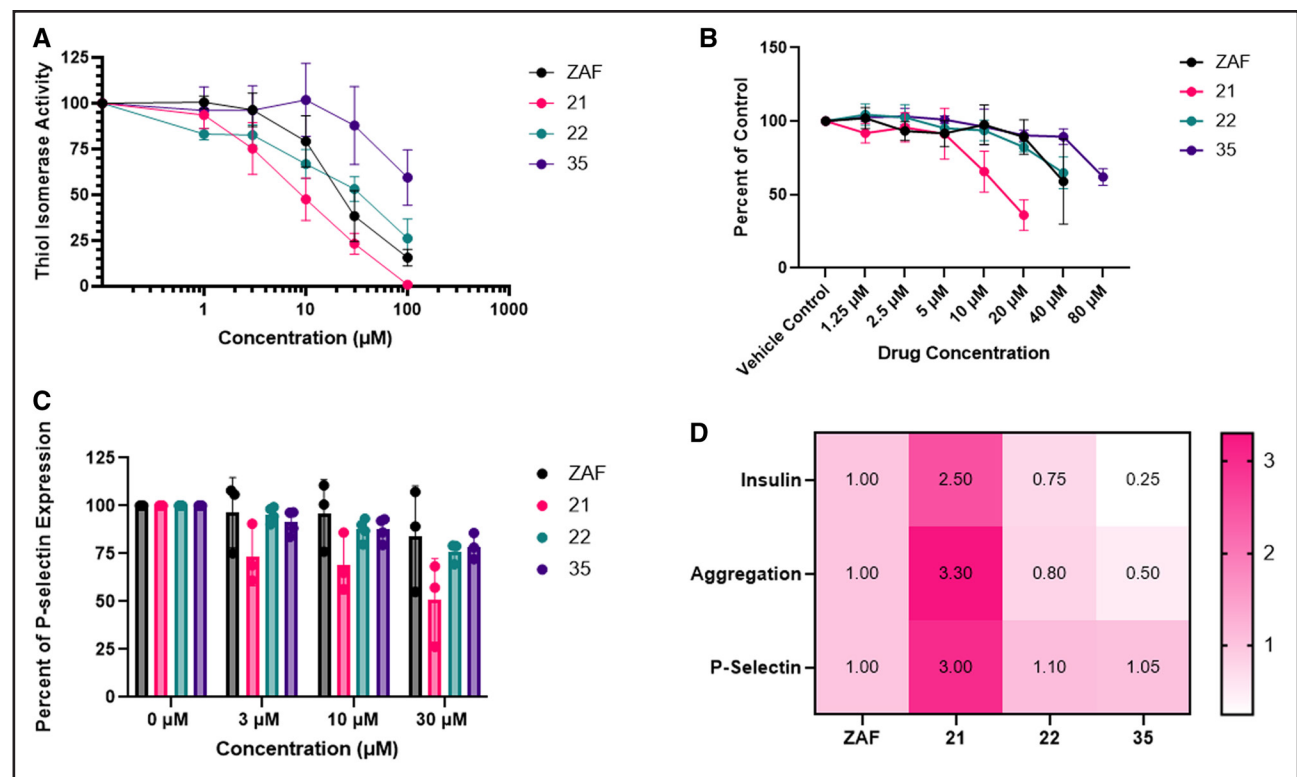


Figure 5. The relative inhibition of the analogues is consistent over multiple assays.

The activity of zafirlukast (ZAF) compared with compounds 21, 22, and 35 in (A) the insulin turbidity assay, (B) platelet aggregation, (C) P-selectin expression, and (D) a summary comparison of the relative activities of each compound.

correlative with their relative thiol isomerase inhibitory activities (Figure 5D).

Inhibition of Platelet Thiols With ZAF and Analogue 21

We previously found that the mechanism by which ZAF inhibited MDA-MB-231 cell migration was by mediation of cell-surface thiols.² To explore whether our observed inhibition of platelet activity was also associated with modulation of platelet-surface thiols, we explored a similar method for platelets. Platelets were washed, treated with either ZAF or compound 21, stimulated with collagen, and then labeled with 3-(*N*-maleimidopropionyl)-biocytin and probed with streptavidin-HRP on an immunoblot to visualize platelet thiols. Compound 21 was significantly more effective at reducing detectable platelet thiols than ZAF when compared with the control. At 20 μmol/L compound 21 demonstrated an average inhibition of 41.8%, while ZAF inhibition averaged 17.4% (Figure 6).

Cytotoxicity Profile of ZAF Analogues

To assess compound safety, we measured the cytotoxicity of ZAF and compound 21 in representative mammalian lung, kidney, and liver cell lines (Figure 7). It was

determined that neither ZAF nor compound 21 displayed cytotoxicity to HEK-293 kidney cells, BEAS-2B lung cells, and HepG2 liver cells at concentrations up to 128 μmol/L.

Inhibition of Arterial Thrombosis With ZAF Analogue 21

We investigated the ability of compound 21 to inhibit arterial thrombosis *in vivo*. Mice were dosed intravenously with either the vehicle control or compound 21, then subjected to laser injury of the cremaster muscle arterioles. Compared with the vehicle control (Figure 8A), thrombus growth was significantly perturbed after treatment with compound 21 (Figure 8B). Analysis of the maximum fluorescence of individual thrombi averaged almost an 80% decrease in animals treated with compound 21 as compared with those mock-treated with the vehicle control (Figure 8C). In our previous study, ZAF treatment decreased the maximum fluorescence by ≈15%, so compound 21 had a stronger effect.² Interestingly, the thrombi formed in animals treated with compound 21 appeared to be significantly less stable than those formed in control animals, as 3-fold more microemboli were identified, signifying thrombi had difficulty forming (Figure 8D). Finally, we assessed the effect that compound 21 had on bleeding times to examine any

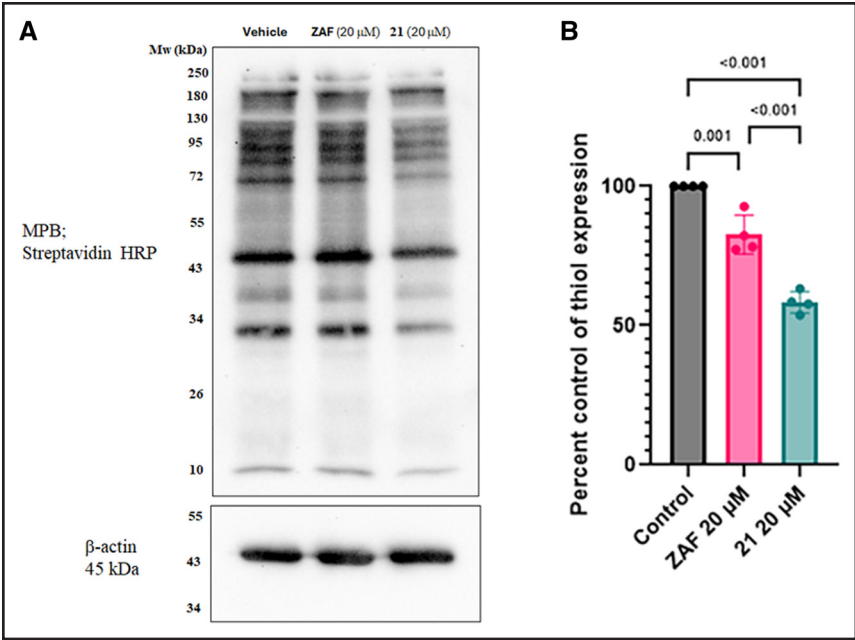


Figure 6. Zafirlukast and compound 21 inhibit free thiols on the platelet surface.
A, Surface thiol labeling with 3-(*N*-maleimidopropionyl)-biocytin (MPB; 100 μ mol/L) from washed platelets treated with zafirlukast (ZAF; $n=4$) or compound 21 ($n=4$). Thiols were detected on immunoblot with streptavidin-HRP (horseradish peroxidase) conjugate (1:5000) and chemiluminescence visualized after addition of enhanced chemiluminescence (ECL) substrate.
B, Quantification of band intensities for surface thiol labeling. Quantification of the total thiols in each lane were calculated using the Image Lab software. Data are presented as mean \pm SD. Statistical analysis: 1-way ANOVA with a Tukey post hoc test.

potential bleeding risk in a murine tail bleed assay. Similar to our previous observations with ZAF, the time to the cessation of tail bleeding was not significantly changed in mice treated with compound 21 (mean, 203 \pm 25 s), compared with mice treated with the vehicle control (mean, 214 \pm 23 s; Figure 8E).

DISCUSSION

In this study, a library of 35 ZAF analogues yielded 1 ZAF analogue 21, which inhibited the thiol isomerase activity of ERp57 more potently than ZAF did and 6 that maintained similar activity to the parent compound.

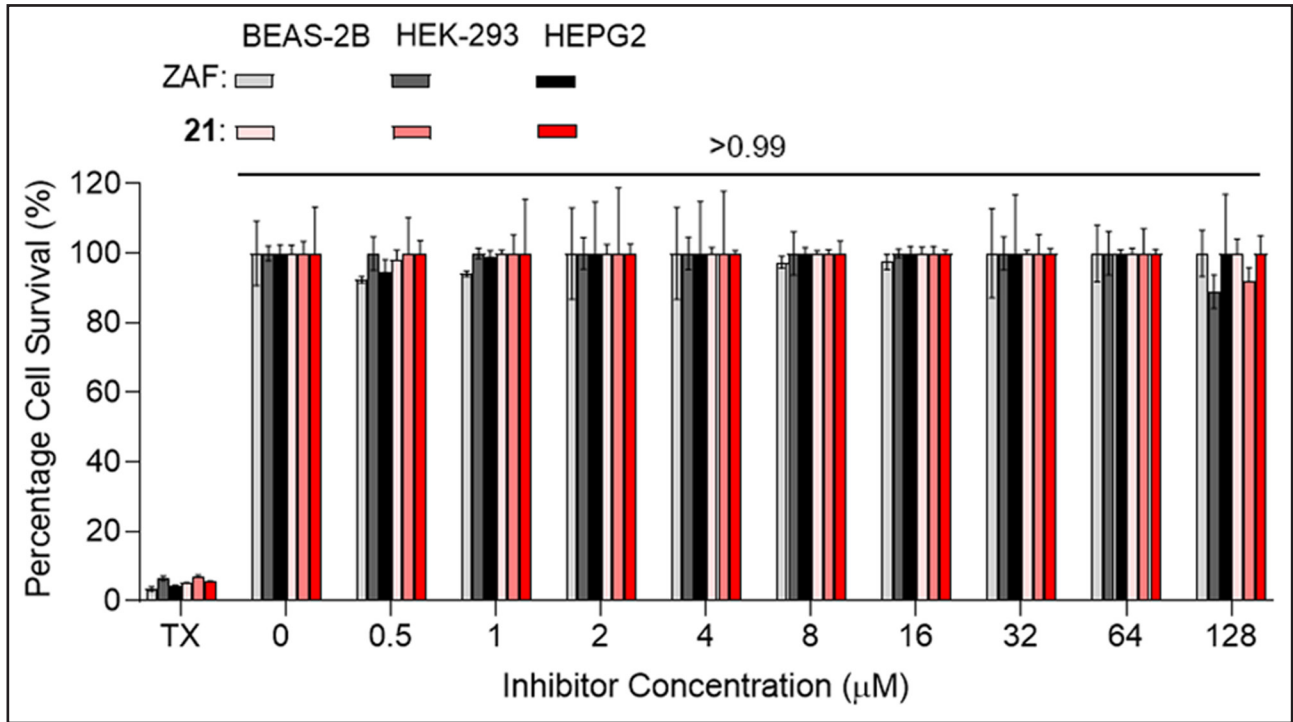


Figure 7. The cytotoxicity of zafirlukast (ZAF) and compound 21 to human bronchial epithelial cells (BEAS-2B), human embryonic kidney cells (HEK-293), and hepatocyte carcinoma (HepG2) cells determined by a resazurin-based assay ($n=4$). The error bars are SDs of the quadruplicate measurements. P values for all positive controls were <0.001 . For BEAS-2B cells, P values for 0.5 μ mol/L ZAF and 1 μ mol/L ZAF were 0.6082 and 0.8435, respectively. For HEK-293 cells, P values for 128 μ mol/L ZAF and compound 21 were 0.1935 and 0.5443, respectively. For HEPG2 cells, the P value for 0.5 μ mol/L ZAF was 0.9093. All other P values were >0.99 . Statistical analysis: 2-way ANOVA with a Dunnett post hoc test.

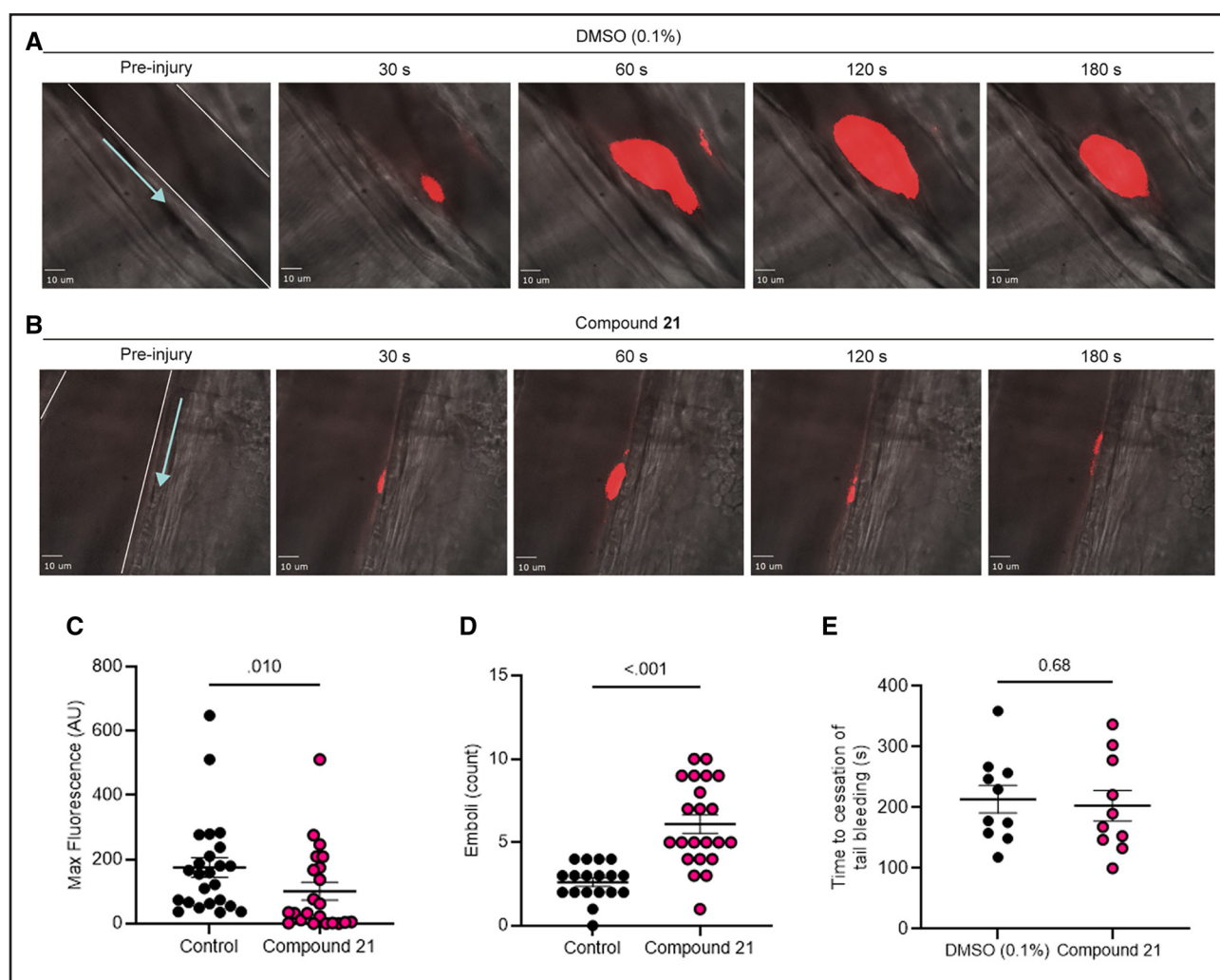


Figure 8. Inhibition of thrombus formation by compound 21 in vivo.

Intravital microscopy using laser injury was performed in male C57BL/6J mice with compound 21 (20 $\mu\text{mol/L}$; $n=5$ mice) or vehicle control (0.1% *v/v* dimethyl sulfoxide [DMSO]; $n=5$ mice) infused intravenously, where multiple thrombi were able to be formed per mouse. **A**, Representative images of thrombi from mice treated with vehicle control at 30, 60, 120, and 180 s. **B**, Representative images of thrombi from mice treated with compound 21 at 30, 60, 120, and 180 s. The white scale bars are 10 mm. The white lines in the preinjury images in **A** and **B** indicate the outline of the vessel, and the turquoise arrows indicate the flow of blood. **C**, The maximum of integrated fluorescence intensity for 0.1% DMSO ($n=24$ thrombi) and compound 21 ($n=22$ thrombi). Data are presented as mean \pm SD. Statistical analysis: Mann-Whitney *U* test. **D**, Measurement of the formation of emboli released from the individual thrombus released in each mouse. Data are presented as mean \pm SD. Statistical analysis: Mann-Whitney *U* test. **E**, The effect of compound 21 on bleeding was assessed via tail bleeding assay where time to cessation of bleeding was recorded after DMSO (0.1%) or compound 21 (20 $\mu\text{mol/L}$) was infused intravenously into C57/BL6 mice for 5 minutes before tail biopsy ($n=10$ per group). Data are presented as mean \pm SD. Statistical analysis: Mann-Whitney *U* test. AU indicates arbitrary units.

Through these studies, we discovered that the presence of the cyclopentyl carbamate group at the C5 position of the indole (ring A) was not needed for the inhibition of ERp57. Future SAR studies with next-generation ZAF analogues will explore ZAF analogues, where the most preferred R_3 substituent on ring C will be kept as 2-F. Compound 21 strongly quenched the Trp fluorescence of ERp57 upon binding. The active domains a and a' of ERp57 contain solvent-exposed Trp residues in their substrate-binding sites,³¹ appearing as likely candidates for direct interactions with compound 21. ZAF and other analogues likely bind to similar sites, but some analogues may permit simultaneous insulin binding at the active

site, which could explain why some analogues appear to be unable to completely inhibit the enzyme. Some of the analogues that inhibited ERp57 incompletely had low IC_{50} values; therefore, these analogues may have favorable structural features for further optimization. Future studies will establish the molecular details of thiol isomerase complexes with ZAF analogues and probe the inhibition mechanism in greater detail, while optimizing the pharmacokinetic parameters previously identified for ZAF for the analogues.^{32,33}

When looking broadly at the data presented in the Table, compounds belonging to scaffold 1 displayed poor activity, while some of those from scaffold 2 displayed

similar or increased activity as inhibitors when compared with the parent ZAF. The higher potency of compound 21 with scaffold 2 indicates that in the context of a substitution pattern distinct from that of ZAF, a cyclopentyl carbamate group at the R₁ position of ZAF is not required for thiol isomerase inhibition. In fact, scaffold 2 (Figure 1), with its 2-methoxy-5-indoyl substituents on ring B, yielded the most active compound 21, which was more potent than ZAF (Table; Figure 2).

Previously, we demonstrated that ZAF was able to inhibit platelet aggregation, P-selectin exposure, and in vivo thrombus formation at physiologically relevant concentrations.² Here, we discovered that the effect of ZAF on platelets could be enhanced with analogue optimization. Compared with ZAF, compound 21 was significantly better at inhibiting platelet aggregation at both 10 and 20 $\mu\text{mol/L}$ and demonstrated inhibition at 10 $\mu\text{mol/L}$ similar to that of ZAF at 40 $\mu\text{mol/L}$ (Figure 4). Importantly, we also established that ZAF and compound 21 inhibited platelet aggregation in PRP, that is, in the presence of plasma proteins, compared with our previous study with ZAF, which used washed platelets,² explaining the observed difference in ZAF's platelet aggregation potency between these 2 studies. Compound 21 demonstrated greater inhibitory effects than we observed with ZAF in our previous study in the in vivo thrombus formation assay (Figure 8), $\approx 80\%$ inhibition of maximum fluorescence, compared with 15% inhibition by ZAF at the same dose.² Taken together, the increased potency of inhibition of platelet function and thrombosis (Figure 4), along with effects that correlate with the relative potencies of analogues for thiol isomerase inhibition (Figure 5), with enhanced inhibition of platelet-surface thiols (Figure 6) suggests that ZAF analogues could further improve the antithrombotic properties of the parent compound.

Although we have demonstrated that ZAF inhibits thiol isomerase activity,^{2,24} and that the inhibition of thiol isomerase activity is linked to the inhibition of thrombus formation,^{9,14,16} it is unknown whether the inhibition of CysLT1 receptor activity contributes to the demonstrated effects of ZAF. Previous studies demonstrated that CysLTR1 is expressed intracellularly and on the cell surface of platelets³⁴ and that CysLTR1 and CysLTR2 both serve as substrates for the leukotriene LTC₄,^{35,36} which has been shown to activate mouse platelets.³⁷ However, the activation of mouse platelets was dependent on CysLTR2,³⁷ whereas ZAF specifically binds the CysLT1 receptor.³⁸ Additionally, in our previous work, the effects of ZAF on integrin-mediated cell migration were measured by the scratch assay both on the cells that expressed CysLTR1 and CysLTR2 (MDA-MB-231), as well as on the cells that did not express these receptors (HEK-293T).² In that study, ZAF prolonged wound closure time in both types of cells, demonstrating that the drug was not working through CysLT-dependent mechanisms. Additionally,

compound 21 has a different scaffold organization from that of ZAF, lacking the cyclopentyl moiety of ZAF that aids its binding to CysLTR. The absence of this moiety reduced ZAF binding to the CysLTR1 receptor by >100 -fold.³⁰ This observation and the additional scaffold differences strongly suggest that the analogue has minimal or no effect on the leukotriene receptor. Finally, compounds 21, 22, and 35, all inhibited platelet aggregation to the extent correlative with their relative thiol isomerase inhibitory activity (Figure 5). Taken together, these data indicate that the effect of ZAF and compound 21 on platelets is due to its effects on thiol isomerase activity while the inhibition of CysLTR1 receptor has minimal or no effect on these processes.

The potential utility of ZAF analogues extends well beyond the field of antithrombotic therapeutics, with applications in cancer and cancer-induced thrombosis, among other diseases.³⁹ We previously demonstrated that ZAF can inhibit tumor growth and tumor metastasis in a xenograft model of ovarian cancer, as well as slowed the rate of rise of a tumor biomarker level in a clinical trial of ovarian cancer.²⁴ As compound 21 proved to be a more potent antithrombotic agent than ZAF, it has a potential to be further developed not only for thrombosis therapy but as a bifunctional antithrombotic and antineoplastic agent. Thiol isomerase inhibitors have also been shown to play important regulatory roles in mast cell regulation and food allergy,⁴⁰ and it would be interesting to see the effect of ZAF analogues lacking the CysLTR1-binding moiety in asthma, considering the known inhibitory effects thiol isomerase inhibition has on IgE.⁴⁰ Several PDI inhibitors structurally distinct from ZAF, including antibiotic bacitracin,^{41,42} bepristat/ML359,^{43,44} the cytotoxic natural product juniferdin,⁴⁴ and the abscisic acid derivative origamicin,⁴⁵ have been identified that are being explored for a multitude of additional disorders and diseases, including neurodegenerative diseases^{45,46} and antiviral agents.^{47–49} These new ZAF analogues could, therefore, serve as new tools for exploring different disease processes.

ARTICLE INFORMATION

Received July 24, 2024; accepted February 10, 2025.

Affiliations

Department of Pharmaceutical and Administrative Sciences, College of Pharmacy and Health Sciences, Western New England University, Springfield, MA (J.A.K., S.E.W., M.K.S., D.R.K.). Institute for Cardiovascular and Metabolic Research, School of Biological Sciences, University of Reading, United Kingdom (J.A.K., K.A.T., S.K., T.S., J.M.G., D.R.K.). Department of Pharmaceutical Sciences, College of Pharmacy, University of Kentucky, Lexington (K.C.H., N.T.C., C.H., O.V.T., S.G.-T.). Department of Medicine, UMass Chan Medical School-Baystate Campus, Springfield (D.R.K.).

Acknowledgments

The authors thank the BioResource Unit staff at the University of Reading for animal care and husbandry and Parvathy Susikumar for helpful discussions on the intravital work. J.A. Keovilay and K.C. Howard drafted the manuscript. K.C. Howard and N.T. Chandrika synthesized the zafirlukast analogues. J.A. Keovilay,

S. Khan, and K.A. Taylor performed the platelet experiments. J.A. Keovilay, M.K. Szahaj, and S.E. Wurl performed the cell-free enzymatic assays. C. Hou performed inhibitor-binding assays. S. Khan and K.A. Taylor performed intravital experiments. T. Sage conducted tail bleeding assays. D.R. Kennedy and J.M. Gibbins designed the experiments. S. Khan, J.A. Keovilay, O.V. Tsodikov, and S. Garneau-Tsodikova prepared the figures. D.R. Kennedy, J.M. Gibbins, S. Garneau-Tsodikova, and O.V. Tsodikov supervised the project, edited the manuscript and supporting information, and provided funding for the work.

Sources of Funding

This work was supported by a National Cancer Institute grant R21CA231000 to D.R. Kennedy, a British Heart Foundation project grant (PG/22/10965) to K.A. Taylor, a British Heart Foundation programme grant (RG/20/7/34866) to J.M. Gibbins as well as a National Institutes of Health (NIH) F31 fellowship DEO29661 to K.C. Howard. J.A. Keovilay and S. Khan were supported by PhD studentships from Quercis Pharma. The content is solely the responsibility of the authors and does not necessarily represent the official views of the NIH.

Disclosures

D.R. Kennedy and J.M. Gibbins are inventors on a patent owned by Western New England University repurposing zafirlukast as a potential antithrombotic medication and receive research funding from Quercis Pharma A.G. D.R. Kennedy and S. Garneau-Tsodikova are also inventors on a patent owned by Western New England University exploring zafirlukast analogues in thrombosis and cancer. The other authors report no conflicts.

Supplemental Material

Figures S1–S2

Major Resources Table

REFERENCES

1. Furie B, Furie BC. Formation of the clot. *Thromb Res*. 2012;130:S44–S46. doi: 10.1016/j.thromres.2012.08.272
2. Holbrook LM, Keeton SJ, Sasikumar P, Nock S, Gelzinis J, Brunt E, Ryan S, Pantos MM, Verbetsky CA, Gibbins JM, et al. Zafirlukast is a broad-spectrum thiol isomerase inhibitor that inhibits thrombosis without altering bleeding times. *Br J Pharmacol*. 2021;178:550–563. doi: 10.1111/bph.15291
3. Stoll G, Kleinschnitz C, Nieswandt B. Molecular mechanisms of thrombus formation in ischemic stroke: novel insights and targets for treatment. *Blood*. 2008;112:3555–3562. doi: 10.1182/blood-2008-04-144758
4. Schorr K. Aspirin and platelets: the antiplatelet action of aspirin and its role in thrombosis treatment and prophylaxis. *Semin Thromb Hemost*. 1997;23:349–356. doi: 10.1055/s-2007-996108
5. Hartwig J, Italiano J Jr. The birth of the platelet. *J Thromb Haemost*. 2003;1:1580–1586. doi: 10.1046/j.1538-7836.2003.00331.x
6. Patel S, Singh R, Preuss CV, Patel N. *Warfarin*. In: StatPearls; 2022.
7. Heit JA. Venous thromboembolism: disease burden, outcomes and risk factors. *J Thromb Haemost*. 2005;3:1611–1617. doi: 10.1111/j.1538-7836.2005.01415.x
8. Sorensen HT, Mellemejaer L, Blot WJ, Nielsen GL, Steffensen FH, McLaughlin JK, Olsen JH. Risk of upper gastrointestinal bleeding associated with use of low-dose aspirin. *Am J Gastroenterol*. 2000;95:2218–2224. doi: 10.1111/j.1572-0241.2000.02248.x
9. Jasuja R, Passam FH, Kennedy DR, Kim SH, van Hessem L, Lin L, Bowley SR, Joshi SS, Dilks JR, Furie B, et al. Protein disulfide isomerase inhibitors constitute a new class of antithrombotic agents. *J Clin Invest*. 2012;122:2104–2113. doi: 10.1172/JCI61228
10. Zwicker JI, Schlechter BL, Stopa JD, Liebman HA, Aggarwal A, Puligandla M, Caughey T, Bauer KA, Kuemmerle N, Wong E, et al; CATIQ Investigators. Targeting protein disulfide isomerase with the flavonoid isoquercetin to improve hypercoagulability in advanced cancer. *JCI Insight*. 2019;4:e125851. doi: 10.1172/jci.insight.125851
11. Flaumenhaft R, Furie B. Vascular thiol isomerases. *Blood*. 2016;128:893–901. doi: 10.1182/blood-2016-04-636456
12. Schulman S, Bendapudi P, Sharda A, Chen V, Bellido-Martin L, Jasuja R, Furie BC, Flaumenhaft R, Furie B. Extracellular thiol isomerases and their role in thrombus formation. *Antioxid Redox Signal*. 2016;24:1–15. doi: 10.1089/ars.2015.6530
13. Furie B, Furie BC. Mechanisms of thrombus formation. *N Engl J Med*. 2008;359:938–949. doi: 10.1056/NEJMra0801082
14. Holbrook LM, Sasikumar P, Stanley RG, Simmonds AD, Bicknell AB, Gibbins JM. The platelet-surface thiol isomerase enzyme ERp57 modulates platelet function. *J Thromb Haemost*. 2012;10:278–288. doi: 10.1111/j.1538-7836.2011.04593.x
15. Holbrook LM, Sandhar GK, Sasikumar P, Schenk MP, Stainer AR, Sahli KA, Flora GD, Bicknell AB, Gibbins JM. A humanized monoclonal antibody that inhibits platelet-surface ERp72 reveals a role for ERp72 in thrombosis. *J Thromb Haemost*. 2018;16:367–377. doi: 10.1111/jth.13878
16. Jordan PA, Stevens JM, Hubbard GP, Barrett NE, Sage T, Authi KS, Gibbins JM. A role for the thiol isomerase protein ERp5 in platelet function. *Blood*. 2005;105:1500–1507. doi: 10.1182/blood-2004-02-0608
17. Essex DW, Li M. Protein disulfide isomerase mediates platelet aggregation and secretion. *Br J Haematol*. 1999;104:448–454. doi: 10.1046/j.1365-2141.1999.01197.x
18. Lahav J, Jurk K, Hess O, Barnes MJ, Farndale RW, Luboshitz J, Kehrel BE. Sustained integrin ligation involves extracellular free sulfhydryls and enzymatically catalyzed disulfide exchange. *Blood*. 2002;100:2472–2478. doi: 10.1182/blood-2001-12-0339
19. Zhou J, Wu Y, Rauova L, Koma G, Wang L, Poncz M, Li H, Liu T, Fong KP, Bennett JS, et al. A novel role for endoplasmic reticulum protein 46 (ERp46) in platelet function and arterial thrombosis in mice. *Blood*. 2022;139:2050–2065. doi: 10.1182/blood.2021012055
20. Wang L, Wu Y, Zhou J, Ahmad SS, Mutus B, Garbi N, Hammerling G, Liu J, Essex DW. Platelet-derived ERp57 mediates platelet incorporation into a growing thrombus by regulation of the alphaIIb beta3 integrin. *Blood*. 2013;122:3642–3650. doi: 10.1182/blood-2013-06-506691
21. Zhou J, Wu Y, Wang L, Rauova L, Hayes VM, Poncz M, Essex DW. The disulfide isomerase ERp57 is required for fibrin deposition *in vivo*. *J Thromb Haemost*. 2014;12:1890–1897. doi: 10.1111/jth.12709
22. Zhou J, Wu Y, Chen F, Wang L, Rauova L, Hayes VM, Poncz M, Li H, Liu T, Liu J, et al. The disulfide isomerase ERp72 supports arterial thrombosis in mice. *Blood*. 2017;130:817–828. doi: 10.1182/blood-2016-12-755587
23. Spector SL. Management of asthma with zafirlukast. Clinical experience and tolerability profile. *Drugs*. 1996;52:36–46. doi: 10.2165/00003495-199600526-00007
24. Gelzinis JA, Szahaj MK, Bekendam RH, Wurl SE, Pantos MM, Verbetsky CA, Dufresne A, Shea M, Howard KC, Tsodikov OV, et al. Targeting thiol isomerase activity with zafirlukast to treat ovarian cancer from the bench to clinic. *FASEB J*. 2023;37:e22914. doi: 10.1096/fj.202201952R
25. Howard KC, Gonzalez OA, Garneau-Tsodikova S. Second generation of zafirlukast derivatives with improved activity against the oral pathogen *Porphyromonas gingivalis*. *ACS Med Chem Lett*. 2020;11:1905–1912. doi: 10.1021/acsmchemlett.9b00614
26. Howard KC, Garneau-Tsodikova S. Selective inhibition of the periodontal pathogen *porphyromonas gingivalis* by third-generation zafirlukast derivatives. *J Med Chem*. 2022;65:14938–14956. doi: 10.1021/acsmchem.2c01471
27. Thamban Chandrika N, Fosso MY, Alimova Y, May A, Gonzalez OA, Garneau-Tsodikova S. Novel zafirlukast derivatives exhibit selective antibacterial activity against *Porphyromonas gingivalis*. *MedChemComm*. 2019;10:926–933. doi: 10.1039/c9md00074g
28. Xu S, Butkevich AN, Yamada R, Zhou Y, Debnath B, Duncan R, Zandi E, Petasis NA, Neamati N. Discovery of an orally active small-molecule irreversible inhibitor of protein disulfide isomerase for ovarian cancer treatment. *Proc Natl Acad Sci USA*. 2012;109:16348–16353. doi: 10.1073/pnas.1205226109
29. Falati S, Patil S, Gross PL, Stapleton M, Merrill-Skoloff G, Barrett NE, Pixton KL, Weiler H, Cooley B, Newman DK, et al. Platelet PECAM-1 inhibits thrombus formation *in vivo*. *Blood*. 2006;107:535–541. doi: 10.1182/blood-2005-04-1512
30. Bernstein PR. Chemistry and structure-activity relationships of leukotriene receptor antagonists. *Am J Respir Crit Care Med*. 1998;157:S220–S225; discussion S225. doi: 10.1164/ajrcm.157.6.mar-3
31. Dong G, Wearsch PA, Peaper DR, Cresswell P, Reinisch KM. Insights into MHC class I peptide loading from the structure of the tapasin-ERp57 thiol oxidoreductase heterodimer. *Immunity*. 2009;30:21–32. doi: 10.1016/j.immuni.2008.10.018
32. Fischer JD, Song MH, Suttle AB, Heizer WD, Burns CB, Vargo DL, Brouwer KL. Comparison of zafirlukast (Accolate) absorption after oral and colonic administration in humans. *Pharm Res*. 2000;17:154–159. doi: 10.1023/a:1007509112383
33. Virchow JC Jr, Prasse A, Naya I, Summerton L, Harris A. Zafirlukast improves asthma control in patients receiving high-dose inhaled corticosteroids. *Am J Respir Crit Care Med*. 2000;162:578–585. doi: 10.1164/ajrcm.162.2.9905041

34. Hasegawa S, Ichiyama T, Hashimoto K, Suzuki Y, Hirano R, Fukano R, Furukawa S. Functional expression of cysteinyl leukotriene receptors on human platelets. *Platelets*. 2010;21:253–259. doi: 10.3109/09537101003615394
35. Lynch KR, O'Neill GP, Liu Q, Im DS, Sawyer N, Metters KM, Coulombe N, Abramovitz M, Figueroa DJ, Zeng Z, et al. Characterization of the human cysteinyl leukotriene CysLT1 receptor. *Nature*. 1999;399:789–793. doi: 10.1038/21658
36. Heise CE, O'Dowd BF, Figueroa DJ, Sawyer N, Nguyen T, Im DS, Stocco R, Bellefeuille JN, Abramovitz M, Cheng R, et al. Characterization of the human cysteinyl leukotriene 2 receptor. *J Biol Chem*. 2000;275:30531–30536. doi: 10.1074/jbc.M003490200
37. Cummings HE, Liu T, Feng C, Laidlaw TM, Conley PB, Kanaoka Y, Boyce JA. Cutting edge: leukotriene C4 activates mouse platelets in plasma exclusively through the type 2 cysteinyl leukotriene receptor. *J Immunol*. 2013;191:5807–5810. doi: 10.4049/jimmunol.1302187
38. Dhaliwal A, Bajaj T. *Zafirlukast*. In: StatPearls; 2024.
39. Powell LE, Foster PA. Protein disulphide isomerase inhibition as a potential cancer therapeutic strategy. *Cancer Med*. 2021;10:2812–2825. doi: 10.1002/cam4.3836
40. Krajewski D, Polukort SH, Gelzinis J, Rovatti J, Kaczinski E, Galinski C, Pantos M, Shah NN, Schneider SS, Kennedy DR, et al. Protein disulfide isomerases regulate IgE-mediated mast cell responses and their inhibition confers protective effects during food allergy. *Front Immunol*. 2020;11:606837. doi: 10.3389/fimmu.2020.606837
41. Essex DW, Li M, Miller A, Feinman RD. Protein disulfide isomerase and sulfhydryl-dependent pathways in platelet activation. *Biochemistry*. 2001;40:6070–6075. doi: 10.1021/bi002454e
42. Lovat PE, Corazzari M, Armstrong JL, Martin S, Pagliarini V, Hill D, Brown AM, Piacentini M, Birch-Machin MA, Redfern CP. Increasing melanoma cell death using inhibitors of protein disulfide isomerases to abrogate survival responses to endoplasmic reticulum stress. *Cancer Res*. 2008;68:5363–5369. doi: 10.1158/0008-5472.CAN-08-0035
43. Bendapudi PKBRH, Lin L, Huang M, Furie B, Flaumenhaft R. ML359, a small molecule inhibitor of protein disulfide isomerase that prevents thrombus formation and inhibits oxidoreductase but not transnitrosylase activity. *Blood*. 2014;124:2880.
44. Khodier C, VerPlank L, Nag PP, Pu J, Wurst J, Pilyugina T, Dockendorff C, Galinski CN, Scalise AA, Passam F, et al. Identification of ML359 as a small molecule inhibitor of protein disulfide isomerase. In: *Probe Reports From the NIH Molecular Libraries Program*. 2010.
45. Ozcelik D, Pezacki JP. Small molecule inhibition of protein disulfide isomerase in neuroblastoma cells induces an oxidative stress response and apoptosis pathways. *ACS Chem Neurosci*. 2019;10:4068–4075. doi: 10.1021/acscchemneuro.9b00301
46. Uehara T, Nakamura T, Yao D, Shi ZQ, Gu Z, Ma Y, Masliah E, Nomura Y, Lipton SA. S-nitrosylated protein-disulphide isomerase links protein misfolding to neurodegeneration. *Nature*. 2006;441:513–517. doi: 10.1038/nature04782
47. Diwaker D, Mishra KP, Ganju L, Singh SB. Protein disulfide isomerase mediates dengue virus entry in association with lipid rafts. *Viral Immunol*. 2015;28:153–160. doi: 10.1089/vim.2014.0095
48. Walczak CP, Tsai B. A PDI family network acts distinctly and coordinately with ERp29 to facilitate polyomavirus infection. *J Virol*. 2011;85:2386–2396. doi: 10.1128/JVI.01855-10
49. Gallina A, Hanley TM, Mandel R, Trahey M, Broder CC, Viglianti GA, Ryser HJ. Inhibitors of protein-disulfide isomerase prevent cleavage of disulfide bonds in receptor-bound glycoprotein 120 and prevent HIV-1 entry. *J Biol Chem*. 2002;277:50579–50588. doi: 10.1074/jbc.M204547200